ISSN 0869-5911, Petrology, 2006, Vol. 14, No. 1, pp. 2–20. © Pleiades Publishing, Inc., 2006.
Original Russian Text © A.M. Larin, A.B. Kotov, E.B. Sal'nikova, V.A. Glebovitskii, M.K. Sukhanov, S.Z. Yakovleva, V.P. Kovach, N.G. Berezhnaya, S.D. Velikoslavinskii, M.D. Tolkachev, 2006, published in Petrologiya, 2006, Vol. 14, No. 1, pp. 4–24.

The Kalar Compex, Aldan–Stanovoi Shield, an Ancient Anorthosite–Mangerite–Charnockite–Granite Association: Geochronologic, Geochemical, and Isotopic–Geochemical Characteristics

A. M. Larin*, A. B. Kotov*, E. B. Sal'nikova*, V. A. Glebovitskii*, M. K. Sukhanov, S. Z. Yakovleva*, V. P. Kovach*, N. G. Berezhnaya*, S. D. Velikoslavinskii*, and M. D. Tolkachev***

**Institute of Precambrian Geology and Geochronology (IGGD), Russian Academy of Sciences, nab. Makarova 2, St. Petersburg, 199034 Russia*
e-mal: alarin@AL7250.spb.edu
***Institute of the Geology of Ore Deposits, Petrography, Mineralogy, and Geochemistry (IGEM), Russian Academy of Sciences, Staromonetnyi per. 35, Moscow, 109017 Russia*
e-mail: anorth@igem.ru

Received November 3, 2004

Abstract—The autonomous (massif-type) anorthosite massifs of the Kalar Complex (2623 ± 23 Ma) intrude high-grade metamorphic rocks of the Kurulta tectonic block at the junction of the Aldan and Dzhugdzhur–Stanovoi fold area. These rocks belong to the most ancient anorthosite–mangerite–charnockite–granite (AMCG) magmatic association, whose origin was constrained to the Mesoproterozoic (1.8–1.1 Ga). The charnockites are typical high-potassium reduced granites like rapakivi, which affiliate with the A type. The Nd and Pb isotopic composition of these rocks suggests their predominantly crustal genesis, whereas the anorthosites were most probably produced by a mantle magma that was significantly contaminated by crustal material at various depth levels. The intrusions of the Kalar Complex were emplaced in a postcollision environment, with the time gap between the collisional event and the emplacement of these massifs no longer than 30 m.y. The southern Siberian Platform includes two definitely distinguished and spatially separated AMCG associations, which have different ages and tectonic settings: (i) the Late Archean (2.62 Ga) postcollision Kalar plutonic complex and (ii) the Early Proterozoic (1.74–1.70 Ga) anorogenic Ulkan–Dzhugdzhur volcano-plutonic complex.

DOI: 10.1134/S0869591106010024

INTRODUCTION

Most ancient cratons typically include large anorthositic plutons, which are classed with *autonomous* anorthosites (Bogatikov, 1979), also referred to as *massif-type* anorthosites (Ashwal, 1993). These anorthosites are commonly associated with A-granites, most typically, rapakivi and charnockites. The studies of such magmatic complexes in Nain and Grenville in Canada and the United States resulted in the recognition of the anorthosite–mangerite–charnockite–granite (AMCG) association, which is regarded as an association of genetically related but not comagmatic igneous rocks (Emslie and Hunt, 1990).

According to (Ashwal, 1993; Wiebe, 1992), massif-type anorthosites occur as intrusive plutons amounting to thousands of square kilometers in area and dominated by massive or weakly layered rocks (anorthosites, leuconorites, leucogabbro, and leucotroctolites), which typically have no volcanic analogues. These rocks are commonly rich in plagioclase (75–95%) of intermediate composition ($An_{50 \pm 10}$), bear anhydrous mineral assemblages, and contain megacrysts of high-Al high-pressure pyroxene. The amount of mafic rocks in these plutons rarely exceeds 10%, and the most differentiated of them are unusual, Fe- and Ti-, and P-rich diorites and jotunites (monzodiorites). The age of massif-type anorthosites is mostly restricted to the Mesoproterozoic (1.8–1.0 Ga).

The granitoids of the AMCG association include rapakivi granites emplaced in hypabyssal and, occasionally, subvolcanic environments, as well as deeper seated mangerites and charnockites (Velikoslavinskii *et al.*, 1978). Frost and Frost (1997) recognized this type as reduced rapakivi-type granites affiliating with the ilmenite series of metaluminous granites. Compared with other A-granites, they are richer in K, HFSE, REE, and F, have the lowest f_{O_2} and f_{H_2O} values and the highest crystallization temperatures, while their Mg–Fe minerals have extremely high Fe#.

The Aldan–Stanovoi Shield is known to include two spatially separated regions with massif-type anorthosites: Kalar in the west and Dzhugdzhur in the east (Fig. 1).

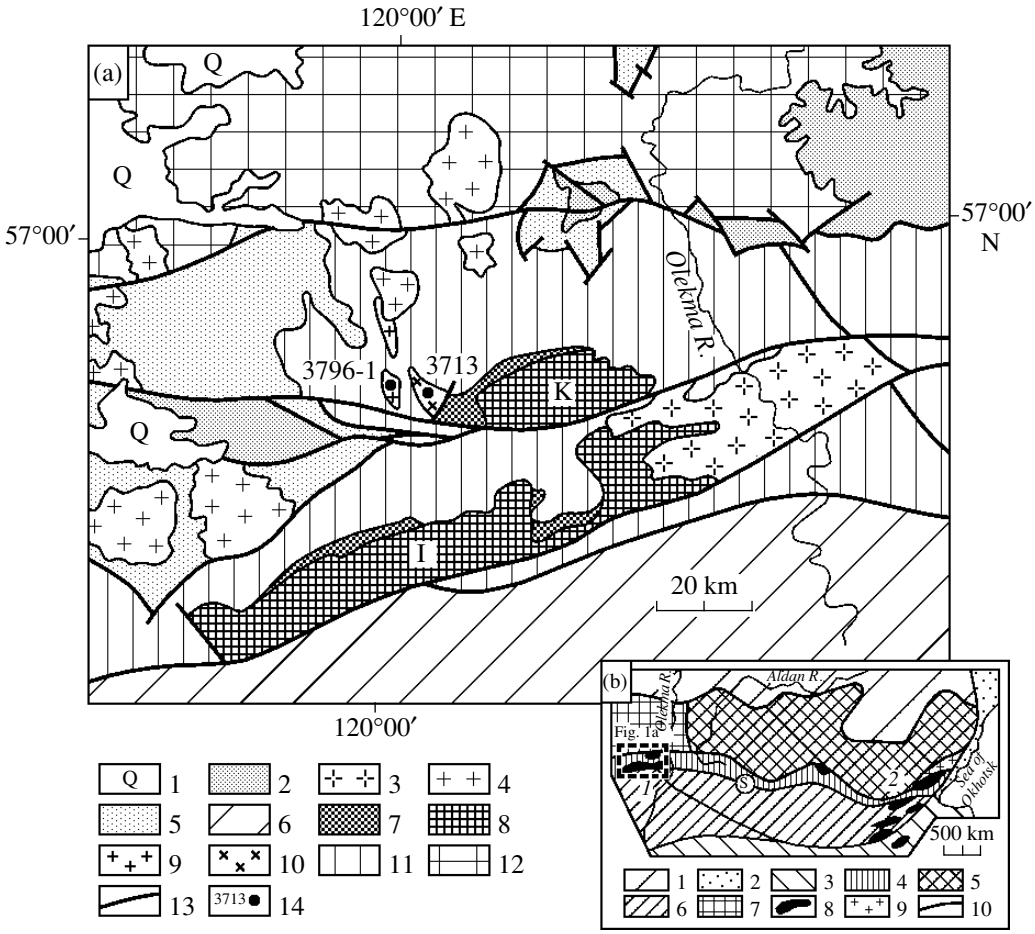

Fig. 1. (a) Schematic geological map of the junction zone of the Chara–Olekma geoblock of the Aldan Shield and Dzhugdzhur–Stanovoi foldbelt.

(1) Quaternary deposits; (2) sedimentary cover of the Siberian Platform; (3) Tass syenite massif (PZ); (4) granite of the Kodar Complex (PR_1); (5) metasedimentary rocks of the Udokan Group (PR_1); (6) Stanovoi Complex of the Dzhugdzhur–Stanovoi foldbelt (PR_1 ?); (7, 8) Kalar Complex (AR_2): (7) charnockites, (8) mafic rocks; (9) charnockites of the Altual'skii Complex (AR_2); (10) enderbites of the Dzheluiskii Complex (AR_2); (11) metamorphic and magmatic rocks of the junction zone between the Chara–Olekma geoblock of the Aldan Shield and Dzhugdzhur–Stanovoi foldbelt (Pristanovoi granulite belt); (12) metamorphic and magmatic complexes of the Chara–Olekma block of the Aldan Shield; (13) faults; (14) sampling site for geochronologic research. Massifs of the Kalar Complex: *I*—Imangakit, *K*—Kuronaakh.

(b) Schematic map showing the location of autonomous anorthosite massifs and related rocks of the Kalar (2.63 Ga) and Dzhugzhur (1.74 Ga) associations in the southern part of the Siberian Platform.

(1) Sedimentary cover of the Siberian Platform; (2) Okhotsk–Chukot volcanic belt; (3) Mongolia–Okhotsk foldbelt; (4) junction zone between the Aldan Shield and Dzhugdzhur–Stanovoi foldbelt (belt of high-pressure granulites); (5) Aldan and Batomgskii geoblocks; (6) Dzhugdzhur–Stanovoi foldbelt; (7) Chara–Olekma geoblock of the Aldan Shield; (8) anorthosites (*1*—Kalar association, *2*—Dzhugdzhur association); (9) anorogenic granites and bimodal volcanic rocks of the Ulkan Complex; (10) major faults (*S*—Stanovoi suture zone).

Some authors (Lennikov, 1979; Moshkin and Dagelaiskaya, 1964) combine them into a single East Asian Anorthosite Belt of Archean age, which extends in a sublatitudinal direction from the Sea of Okhotsk to eastern Transbaikalia.

The studies of the Dzhugdzhur anorthosites have revealed that these rocks are not Archean (as was thought previously) but Early Proterozoic (1736 ± 6 Ma; Neymark *et al.*, 1992). Moreover, it was determined that the rocks of the Ulkan volcanic complex, which accompany the anorthosites are syngenetic with them, and also belong to the AMCG association (1736–1705 Ma; Larin *et al.*, 1997).

The dates obtained over the past decades for the Kalar Complex by a variety of geochronologic techniques (U–Pb, Rb–Sr, and Sm–Nd) lie within the range of 2.7–1.7 Ga (Vinogradov *et al.*, 1983; Levchenkov *et al.*, 1987; Sukhanov and Zhuravlev, 2002). The contradictory character of these data led the authors to revise them with the use of U–Pb zircon dating. Our research has revealed that the Kalar Complex has an age of 2623 ± 23 Ma, and the age of the overprinted

high-grade metamorphism is 1849 ± 15 Ma (Sal'nikova *et al.*, 2004a).

The affiliation of the Dzhugdzhur anorthosites to the AMCG association is not doubted any more (Larin *et al.*, 1997). The anorogenic tectonic setting of the Ulkan–Dzhugdzhur AMCG association is also quite certain (Larin *et al.*, 1997; Larin, 2004). At the same time, it is still not fully clear whether the anorthosites of the Kalar Complex and associated rocks do belong to the AMCG association and what is their tectonic setting. Moreover, the scope of the Kalar Complex is also disputable. Some researchers (Priyatkina and Lavrovich, 1985; Levchenkov *et al.*, 1987) believe (in our opinion, without any sound grounds for it) that the scope of the complex can be extended by including genetically foreign rocks, for example, charnockites of metamorphic genesis. Because of this, the principal tasks of our research were as follows:

(1) to determine the U–Pb zircon age of the enderbites and charnockites of the Kurulta block (the affiliation of these rocks with the Kalar Complex is questioned);

(2) to obtain geochemical and isotopic–geochemical data (Nd, Pb) to elucidate the sources of the magmatic rocks of the Kalar Complex;

(3) to determine whether the rocks of the Kalar Complex do actually belong to the AMCG magmatic association;

(4) to identify the tectonic setting of the Kalar Complex.

GEOLOGY OF THE KALAR COMPLEX

The Kalar Complex comprises two closely spaced and sublatitudinal anorthosite massifs: Kuronaakh and Imangakit, which are hosted by the Kurulta and Kalar blocks in the junction zone of the Aldan Shield and the Dzhugdzhur–Stanovoi Foldbelt (Fig. 1). The massifs are gently sloping (northward) tabular bodies up to 3–4 km thick and 50–120 km long. The host rocks are migmatized (charnockite-migmatites) garnet–biotite (±sillimanite, ±hypersthene) plagiogneisses of the Kurulta Formation, which contain occasional layers of two-pyroxene crystalline schists, calc-silicate rocks, quartzites, and magnetite quartzites. The contacts between the anorthosites and their host rocks are usually tectonic, although eruptive relations were also encountered and were marked by outer-contact hornfels zones (Priyatkina and Lavrovich, 1985).

The massif of the Kalar Complex are zonal and are dominated by anorthosites, which grade into coarsely layered melanocratic mafic rocks in the margins of the massif. The anorthosites are associated with charnockites of two types (Sukhanov and Vaganov, 1991). The charnockites of the first type compositionally approximate quartz monzonites and quartz syenites and are localized exclusively along the northern contacts of the massif and compose elongated bodies conformable with the anorthosites. The charnockites of the second type correspond to granites in composition and mark the outer contour of the massif or occur as small individual bodies, nearly conformable with their host rocks, not far from the massifs. The contacts between the charnockites and their host rocks and anorthosites are usually intrusive (Bazhenova, 1974), although sometime the anorthosites and charnockites are related through zones of gradual transitions (Sukhanov and Vaganov, 1991). Most researchers ascribe these charnockites to the Kalar Complex (Bazhenova, 1974; *Magmatic Rocks*, 1985; Priyatkina and Lavrovich, 1985; Sukhanov and Vaganov, 1991).

The Kalar Complex is dominated by anorthosites, whose primary magmatic textures remain preserved only in the central parts of the massifs. Depending on the metamorphic grade, the composition of the plagioclase varies form labradorite to oligoclase, and the most common anorthosite varieties contain andesine (Bazhenova, 1974; Sukhanov, 1984). Oligoclase anorthosites, which were produced during the late diaphthoresis (Bazhenova, 1974; Sukhanov, 1984; Sukhanov and Vaganov, 1991), occur mostly within the Stanovoi Fault zone. The predominant mafic mineral of the anorthosites is hypersthene, which is of obviously metamorphic genesis. Inverted pigeonite is more rare. It is a relict mineral of the primary magmatic assemblage (Sukhanov, 1984). The pigeonite is sometimes associated with clinopyroxene of the augite-pigeonite solid solution. The anorthosites also contain secondary hornblende and garnet porphyroblasts.

The rocks of the marginal complex are gabbro-anorthosites, gabbro-norites, gabbro, jotunites, and more rare ultramafic rocks. The mineralogical composition of the gabbroids is generally identical to that of the anorthosites. The ultramafic rocks contain forsterite. The jotunites bear plagioclase of composition $An_{35–45}$ with an antiperthitic structure, orthopyroxene, augite, and apatite. The intercumulus minerals are titanomagnetite, ilmenite, mesoperthite, brown biotite, and, sometimes, also quartz (*Magmatic Rocks*, 1985). The melanocratic marginal complex is known to host deposits of apatite–ilmenite–titanomagnetite ores.

The charnockites of the Kalar Complex consist of augite, hypersthene, hastingsite, brown biotite, fayalite, perthite, antiperthitic plagioclase (oligoclase), and quartz. The Fe–Mg minerals typically have high Fe#. Fayalite was found only in the type-I charnockites, which crystallized at P = 7–8 kbar. All rocks of the Kalar Complex were metamorphosed to the granulite facies of moderate pressure (6–7 kbar) and suffered diaphthoresis to the greenschist facies (*Magmatic Rocks*, 1985).

Along with the charnockites, which are usually thought to compose a single magmatic association with the mafic rocks of the Kalar Complex, the Kurulta block contains widespread enderbite and charnockite massifs of the Dzheluiskii and Altual'skii complexes, which were emplaced before the Kalar Complex was

formed, apparently synchronously with the granulite-facies metamorphism (Shemyakin and Kotov, 1985; Kotov and Samorukova, 1990).

The Dzheluiskii Complex comprises a number of relatively small massifs (Fig. 1) that consist of enderbites. These rocks are made up of hypersthene, biotite, plagioclase, and quartz and sometimes contain significant amounts of clinopyroxene and potassic feldspar. Their composition varies from quartz diorite to granite. Although the enderbites were affected by extensive overprinted structural–metamorphic alterations, their primary intrusive relations with the host rocks can be discerned in places. At the same time, the enderbite of the complex in question were protolithic rocks for the charnockite migmatites, a fact that constrains the position of these rocks in the structural–temporal chart.

The charnockites of the Altual'skii Complex compose massifs up to 100–120 km^2 in area (Fig. 1), which typically have intrusive relations with the rocks of the Kurulta Formation. The composition of the charnockites varies from quartz monzonite to leucogranite, and these rocks consist of hypersthene, diopside, high-Fe amphibole (ferrohastingsite), biotite, plagioclase, potassic feldspar, and quartz.

ANALYTICAL TECHNIQUES

Rocks were analyzed for major elements by XRF and for trace elements by XRF (Rb, Sr, Y, Zr, Nb, Th, Ba, Sr, Co, Ni, and V) or ICP-MS (REE, Zn, Y, Nb, Hf, Ta, Th, and U) accurate to 5–10%.

Accessory zircon was extracted from rocks following the conventional technique with the use of heavy liquids. The U–Pb isotopic studies were conducted with relatively large (0.4–1.0 mg) and small (10–50 zircon grains) samples, as well as with single zircon grains that had been preliminarily air-abraded (Krogh, 1982). The inner structure of individual zircon grains was examined under an optical microscope and with the use of cathodoluminescence (CLC method; Poller *et al.*, 1997). In the latter method, the U–Pb dating was accomplished on one-half of a zircon grain that was extracted from the sample for cathodoluminescence. The selected zircon crystal was subjected to the stepwise removal of its surface contamination in alcohol, acetone, and 1M HNO_3. After each stage, the zircon grain or its fragment was washed in analytically pure water. The decomposition of the material and the chemical extraction of Pb and U were conducted by the modified method (Krogh, 1973). The blank during the experiment did not exceed 50 pg for Pb and 5 pg for U. The Pb and U isotopic compositions were determined on a Finnigan MAT-261 mass spectrometer, in static mode, with the use of an electronic multiplier (the discrimination coefficient for Pb was 0.32 ± 0.11 a.m.u.). The raw experimental data were processed with the PbDAT (Ludwig, 1991) and ISOPLOT (Ludwig, 1999) computer programs. In calculating the age values, we used conventional decay constants for U (Steiger and Jager, 1976). Corrections for common Pb were introduced in compliance with the model values (Stacey and Kramers, 1975). All errors are reported for a 2σ level.

The method of the Sm–Nd isotopic research was described in (Neymark *et al.*, 1993). The blanks were 0.03–0.2 ng for Sm and 0.1–0.5 ng for Nd. The measured $^{143}Nd/^{144}Nd$ ratios were normalized to $^{146}Nd/^{144}Nd = 0.7219$ and brought to the ratios of $^{143}Nd/^{144}Nd = 0.511860$ in the LaJolla Nd standard. The accuracy of the analyses for Sm and Nd was ±0.5%, and the isotopic ratios were measured accurate to ±0.5% for $^{147}Sm/^{144}Nd$ and to 0.005% for $^{143}Nd/^{144}Nd$ (2σ). The weighted mean values of the $^{143}Nd/^{144}Nd$ ratio in the LaJolla Nd standard (average of eleven measurements) was 0.511874 ± 8 (2σ). In calculating the values of $\varepsilon_{Nd}(0)$ and model ages $T_{Nd}(DM)$, we used the modern values for CHUR $^{143}Nd/^{144}Nd = 0.512638$ and $^{147}Sm/^{144}Nd = 0.1967$ from (Jacobsen and Wasserburg, 1984) and for DM $^{143}Nd/^{144}Nd = 0.513151$ and $^{147}Sm/^{144}Nd = 0.2136$ (Goldstein and Jacobsen, 1988). The two-stage model ages $T_{Nd}(DM\text{-}2st)$ (Liew and Hofmann, 1988) were calculated using the value of $^{147}Sm/^{144}Nd = 0.12$ (Taylor and McLennan, 1985).

The Pb–Pb isotopic study of feldspar was conducted by the method described in (Neymark *et al.*, 1993). The plagioclase samples were preliminarily treated with 0.01 N HCl and then powdered. The powders were then treated with 15 N HNO_3 for 5–6 h at heating to remove radiogenic Pb. Both the acid leachates and the leaching residues were examined. The blank was 0.4 ng for Pb. The Pb isotopic composition was measured on a Finnigan MAT-261 mass spectrometer. The precision of the Pb isotopic analysis is controlled by mass fractionation. The fractionation coefficient $f = 0.0013 \pm 0.0002$ a.m.u.$^{-1}$ was determined by multiple measurements of the NBS-SRM-982 isotopic standard. The model parameters were calculated by the ISOPLOT computer program (Ludwig, 1991a).

GEOCHEMISTRY

Both the mafic and acid rocks of the complex belong to the subalkaline series. The former are characterized by low concentrations of most incompatible elements (except Sr and Ba) (Tables 1, 2, Fig. 2), even as compared with the analogous rocks of other AMCG associations. The anorthosites additionally have very low concentrations of compatible elements, contain very small concentrations of REE, whose patterns are generally typical of massif-type anorthosites and principally differ from those of the other anorthosite type: Archean megacrystic anorthosites (Ashwal, 1993; Wiebe, 1992). The REE patterns of the basic rocks of the Kalar Complex are typically enriched in LREE and have pronounced positive Eu anomalies (Table 2, Fig. 3). The jotunites differ from other melanocratic rocks in having higher concentrations of Fe, Ti, P, K, Ba, Zr, Hf, Ta, and

Table 1. Chemical composition of magmatic rocks of the Kalar Complex and host granitoids

Component	Kalar Complex								Synmetamorphic charnockites and enderbites			
	Kuronaakh Massif				Imangakit Massif				Dzheluiskii Massif		Altual'skii Massif	
	KA-12	KA-13	KA-4	1267*	A-80-1*	203-8*	203-10*	8013-7*	3706	3713	3796-1	3905
	Anorthosite	Anorthosite	Gabbro	Charnockite I	Anorthosite	Charnockite I	Charnockite I	Charnockite II	Enderbite	Enderbite	Charnockite	Charnockite
SiO_2	54.6	53.19	48.7	62.14		60.73	63.16	71.31	69.70		71.65	71.42
TiO_2	0.09	0.42	1.3	0.85		1.09	1.06	0.45	0.37		0.25	0.40
Al_2O_3	25.1	25.34	18.4	13.85		15.59	13.79	13.26	15.45		14.01	12.78
Fe_2O_3	2.00	4.01	14.4	10.07		2.60	2.62	1.12	1.45		0.94	2.35
FeO						7.78	7.85	3.36	1.89		1.96	2.46
MnO	0.02	0.05	0.16	0.18		0.14	0.11	0.04	0.04		0.04	0.05
MgO	0.98	1.91	4.5	0.53		0.60	0.75	0.20	1.33		0.88	0.47
CaO	10.5	9.03	7.6	3.24		3.96	2.96	1.50	3.71		1.18	1.89
Na_2O	5.50	4.89	3.80	3.99		3.38	3.13	3.38	4.73		3.65	3.52
K_2O	0.43	0.53	0.33	4.21		2.99	3.42	4.56	1.18		5.31	4.54
P_2O_5	0.053	<0.05	0.16	0.22		0.16	0.13	0.04	0.14		0.14	0.13
LOI	<0.30	0.70	<0.30	0.20		0.50	0.80	0.40	0.55		0.57	0.41
Rb	2.6	3.5	3.1	21	10	45	96	158	20.6	52.1	65.6	35.3
Ba	230	361	211	320	420	3510	4615	1545	361	2238	896	2919
Sr	485	437	372	235	620	685	405	125	453	220	103	209
Zr	4.3	7.1	14.7	3145	30	720	1495	850	101	91.8	212	345
Hf	0.17	0.22	0.44	55.80	0.65	23.0	41.4	16.0	2.45	2.42	5.55	7.33
Y	0.85	2.39	4.90						3.54	21.07	29.86	18.87
Ta	0.02	0.06	0.08	1.70		0.65	1.10	2.05	0.17	0.60	0.40	0.41
Nb	0.47	0.95	1.80						4.56	14.26	14.20	11.21
Th	0.15	0.37	0.13	3.13	0.70	3.36	2.35	13.30	3.56	1.17	10.00	2.10
U	0.02	0.06	0.05	2.66		1.33	1.75	1.34	0.22	0.34	0.37	0.23
Cr	52	269	323	28	18	17	36	15	23	18	31	14
Co	12	18	63	23	10	6	13	3	6	3	2	2
Ni	19	52	206	54		5		45	19	14	19	6
V	10	53	195						22	3	3	<1
Zn	5.22	27.63	107.0						47.03	44.50	36.84	47.95

Note: Oxides are given in wt %, elements in ppm.
* Analytical data are form (Sukhanov and Vaganov, 1991).

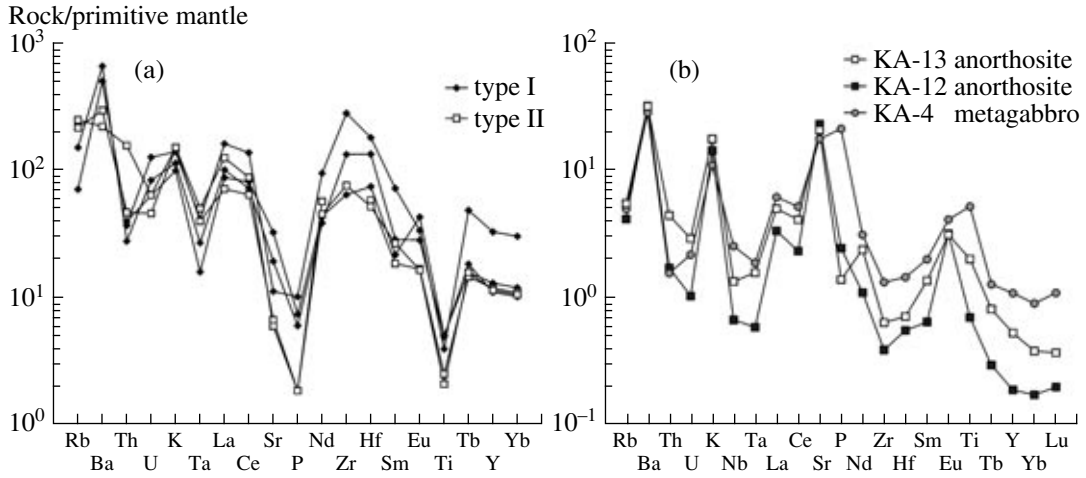

Fig. 2. Fractionation of incompatible elements in rocks of the Kalar Complex.
(a) Charnockites, (b) mafic rocks. Primitive mantle is after (Sun and McDonough, 1989).

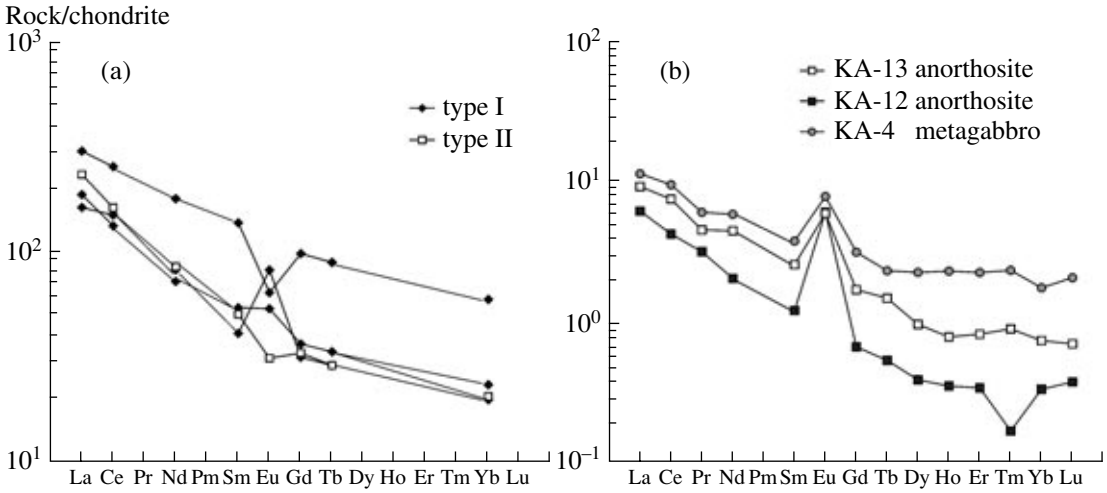

Fig. 3. Chondrite-normalized (Taylor and McLennan, 1985) REE patterns for rocks from the Kalar Complex.
(a) Charnockites, (b) mafic rocks.

REE at lower contents of Cr, Ni, and Co (Sukhanov and Vaganov, 1991).

The charnockites of the Kalar Complex affiliate with the calc–alkaline series. The proportions of alkalis in the charnockites of elevated alkalinity are roughly similar, but the enrichment of these rocks in SiO_2 is associated with their predominant enrichment in K_2O. These rocks are usually highly ferrous, FeO*/(FeO* + MgO) > 0.9. The occurrence of relics of primary magmatic fayalite and the virtual absence of magnetite testify that they belong to reduced rapakivi-type granites (Frost and Frost, 1997). These charnockites are commonly high in HFSE, LREE, and Ba. The spidergrams in Fig. 2 demonstrate that the type-I charnockites have negative anomalies at Rb, Ta, Th, Sr, Ti, and P and positive anomalies at Ba, Zr, and Hf. The type-II charnockites are more differentiated that the analogous rocks of type I. They also typically have high concentrations of K, Rb, Th, and Th but are poorer in Ba, Sr, P, Zr, Hf, and HREE. The REE patterns of the type-I charnockites (Fig. 3) show an enrichment in LREE [$(La)_N$ = 302–163, $(Yb)_N$ = 60–20, $(La/Yb)_N$ = 9.3–5.0), moderately fractionated LREE and MREE [$(La/Sm)_N$ = 3.9–2.2], and relatively strongly fractionated MREE and HREE [$(Gd/Yb)_N$ = 1.8–1.3]. The least differentiated type-I charnockites have positive Eu anomalies (Eu/Eu* = 1.2–2.3). These rocks are usually poor in K_2O and have the highest concentrations of Ba and Sr. These geochemical features were most probably caused by the presence of cumulus plagioclase. The most differentiated charnockites of this type are noted for high concentrations of K, REE, and HFSE and extremely

Table 2. REE concentrations (ppm) of magmatic rocks of the Kalar Complex and host granitoids

Component	Kalar Complex							Synmetamorphic charnockites and enderbites			
	Kuronaakh Massif				Imangakit Massif			Dzheluiskii Massif		Altual'skii Massif	
	KA-12	KA-13	KA-4	1267*	203-10*	203-8*	8013-7*	3706	3713	3905	3796-1
	Anorthosite	Anorthosite	Gabbro	Charnockite I	Charnockite I	Charnockite I	Charnockite II	Enderbite	Enderbite	Charnockite	Charnockite
	ICP MS**	ICP MS	ICP MS	INA	INA	INA	INA	ICP MS	ICP MS	ICP MS	ICP MS
La	2.29	3.42	4.21	111.00	69.00	60.00	86.00	23.15	37.19	61.53	50.24
Ce	4.11	7.25	9.16	244	128	144	156	42.92	74.77	95.81	165
Pr	0.44	0.63	0.84					4.37	8.78	12.65	13.91
Nd	1.48	3.21	4.21	128.00	52.00	59.00	61.00	14.75	35.45	46.51	52.22
Sm	0.28	0.60	0.88	32.00	12.70	9.60	11.80	1.96	6.03	7.25	9.20
Eu	0.53	0.52	0.69	5.63	4.73	7.2	2.76	0.66	2.92	3.41	1.37
Gd	0.21	0.53	0.98					1.60	5.51	5.98	8.30
Tb	0.03	0.09	0.14	5.22	1.97	1.70	1.70	0.16	0.83	0.84	1.17
Dy	0.15	0.37	0.87					0.68	4.15	4.11	6.44
Ho	0.03	0.07	0.20					0.14	0.85	0.78	1.21
Er	0.09	0.21	0.57					0.35	2.18	2.18	3.18
Tm	0.01	0.03	0.08					0.06	0.31	0.28	0.43
Yb	0.08	0.19	0.44	14.90	5.00	5.88	5.18	0.37	1.97	1.97	2.58
Lu	0.01	0.03	0.08					0.05	0.29	0.31	0.35
$[La/Yb]_N$	18.32	12.40	6.44	5.03	9.32	6.90	11.22	42.5	12.74	21.12	13.14
$[La/Sm]_N$	5.06	3.59	3.00	2.18	3.42	3.93	4.59	7.43	3.88	5.34	3.44
$[Gd/Yb]_N$	2.00	2.30	1.79	1.65	1.83	1.35	1.60	3.51	2.64	2.46	2.60
Eu/Eu*	6.69	2.83	2.26	0.55	1.20	2.27	0.77	1.15	1.55	1.58	0.48

* Analytical data are form (Sukhanov and Vaganov, 1991).
** Analytical technique.

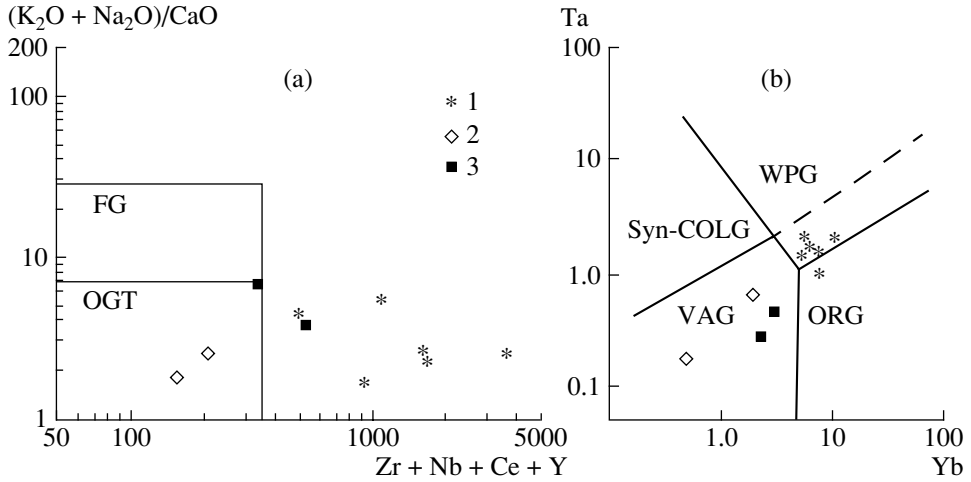

Fig. 4. Geochemical discriminant diagrams for felsic rocks.
(a) $(Na_2O + K_2O)/CaO$ vs. (Zr + Nb + Ce + Y) diagram (Whalen *et al.*, 1987). (b) Ta vs. Yb diagram (Pearce *et al.*, 1984). Fields: OGT—unfractionated M-, I-, and S-type granites; FG—fractionated felsic granites; ORG—ocean ridge granites; Syn-COLG—syn-collisional granites; VAG—volcanic arc granites; WPG—within plate granites.
Magmatic complexes: (1) Kalar, (2) Dzheluiskii, (3) Altual'skii.

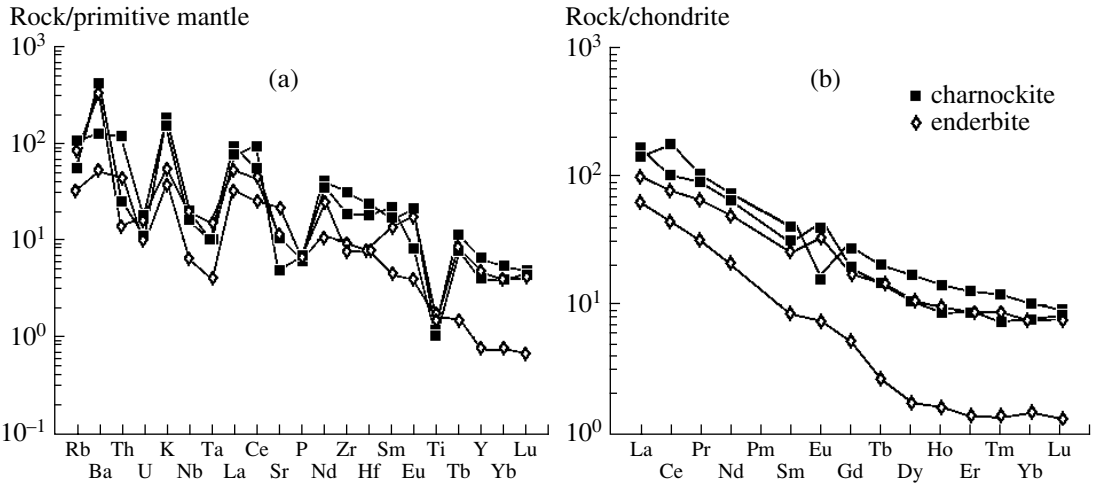

Fig. 5. Geochemical diagrams for enderbites from the Dzheluiskii Complex and charnockites from the Altual'skii Complex.
(a) Fractionation of incompatible elements relative to the primitive mantle (Sun and McDonough, 1989); (b) chondrite-normalized (Taylor and McLennan, 1985) REE patterns.

low contents of Ba and Sr. The REE patterns display HREE enrichment [$(La/Yb)_N$ = 5.0, $(Yb)_N$ = 60] and negative Eu anomalies (Eu/Eu* = 0.55). The REE patterns of the type-II charnockites are generally similar to the patterns of the type-I charnockites and differ from them by stronger fractionation [$(La/Yb)_N$ = 11.2, $(La/Sm)_N$ = 4.6].

In discriminant geochemical diagrams (Fig. 4), the charnockites of the Kalar Complex plot within the field of within-plate A-granites. The geochemistry of these rocks is practically identical to that of Late Proterozoic charnockites of the AMCG association in the Grenville province and the Rogoland Complex in Norway (Higgins and van Breemen, 1996; Bolle *et al.*, 2003).

The andesites of the Dzheluiskii Complex and the charnockites of the Altual'skii Complex are geochemically similar and principally differ from the charnockites of the Kalar Complex (Tables 1, 2, Figs. 4, 5). They are characterized by much broader compositional variations. In a $(K_2O + Na_2O - CaO)$ vs. SiO_2 diagram, the compositions of these rocks vary from the calc–alkaline to calc series. The rocks have moderate or relatively low Fe#: 0.84 for the charnockites and 0.72 for the enderbites. All of these rocks are notably depleted in incompatible elements, particularly HFSE (Fig. 5)

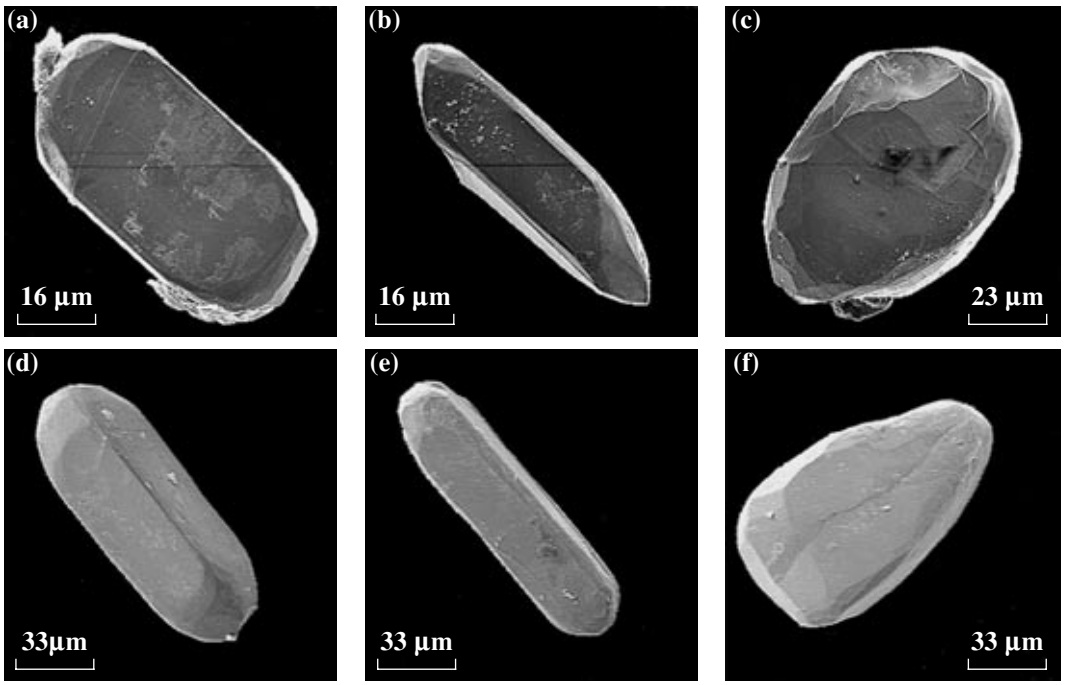

Fig. 6. SEM images of zircon grains [ABT scanning electron microscope, 20 kV accelerating voltage; (a–c) sample 3713; (d–f) sample 3796-1] and SEM images of zircon grains [CamScan scanning electron microscope equipped with a cathodoluminescence detector, 15 kV accelerating voltage; (g–i) sample 3713; i—CLC no. 7 in Table 1; (j, k) sample 3796-1, type I, (l, m) type II, (n–p) type I. CLC no. 15 in Table 1; (q–s) type III].

compared to the charnockites of the Kalar Complex. The REE patterns (Fig. 5) are strongly fractionated [$(La/Yb)_N$ = 12.7–42.5], particularly for LREE [$(La/Sm)_N$ = 3.4–7.4, $(Gd/Yb)_N$ = 2.3–3.5]. The rocks have insignificant positive or, sometimes, negative Eu anomalies (Eu/Eu* = 1.58–0.48). In discriminant tectono-magmatic and geochemical diagrams (Fig. 4), these rocks plot within the fields of granites from magmatic arcs. The most primitive enderbite (sample 3706) is geochemically close to the Archean rocks of the TTG association (Condie, 1993; Martin, 1994).

U–Pb GEOCHRONOLOGY

The U–Pb geochronologic study was conducted on enderbites (biotite–hypersthene granodiorite) of the Dzheluiskii Complex (sample 3713) and charnockites (biotite–hypersthene subalkaline granite) of the Altual'skii Complex (sample 3796-1). The sampling sites of these rocks are displayed in Fig. 1.

The sample of accessory zircon separated from the Dzheluiskii enderbite consisted of subhedral transparent and semitransparent long- or short-prismatic crystals (Figs. 6a–6c) of pale pink and pinkish cherry color. The crystals show {100} and {110} prisms and {101}, {111}, {201}, and {011} dipyramids. In transmitted light, these zircon grains exhibit traces of primary magmatic zoning and growth zones rich in mineral inclusions. Their zoning is also visible in cathodoluminescence (CL) (Figs. 6g–6i). The crystals have patches characterized by strong luminescence, which occur in both crystal margins and cores. Moreover, some of the crystals contain relict inherited cores (Fig. 6h). The zircon grains range from 50 to 300 μm, and their K_{elong} = 1.9–6.0.

Initially, the isotopic research was conducted with relatively large (0.6–1 mg) samples of the "purest" zircon grains of pinkish cherry color, which were separated from the size fractions +70–80 μm and >150 μm (Table 3, nos. 1, 2). This zircon appeared to have discordant U/Pb ratios (Table 3, Fig. 7). In order to minimize its discordance, we subjected the mineral to air abrasion and acid treatment (Mattinson, 1994). Upon air abrasion, we selected single zircon grains for dating; the selection was accomplished based on the results of optical examination (Table 3, nos. 3 and 4) and cathodoluminescent monitoring (Table 3, no. 7) of the inner structures of the grains (CLC method; Poller *et al.*, 1997). The data points of the zircon residue after its acid treatment (Table 3, Fig. 7, nos. 5, 6) and the point of untreated zircon from the >150 μm fraction define a discordia (Fig. 7), whose upper intercept corresponds to an age of 2627 ± 16 Ma, and the lower intercept corresponds to 1688 ± 75 Ma (MSWD = 0.74). The isotopic composition points of zircon from the small fraction and this mineral after air abrasion plot slightly away to the right of the discordia, most probably because of the presence of relict cores that sometimes cannot be discerned in transmitted light. The zircon grain selected

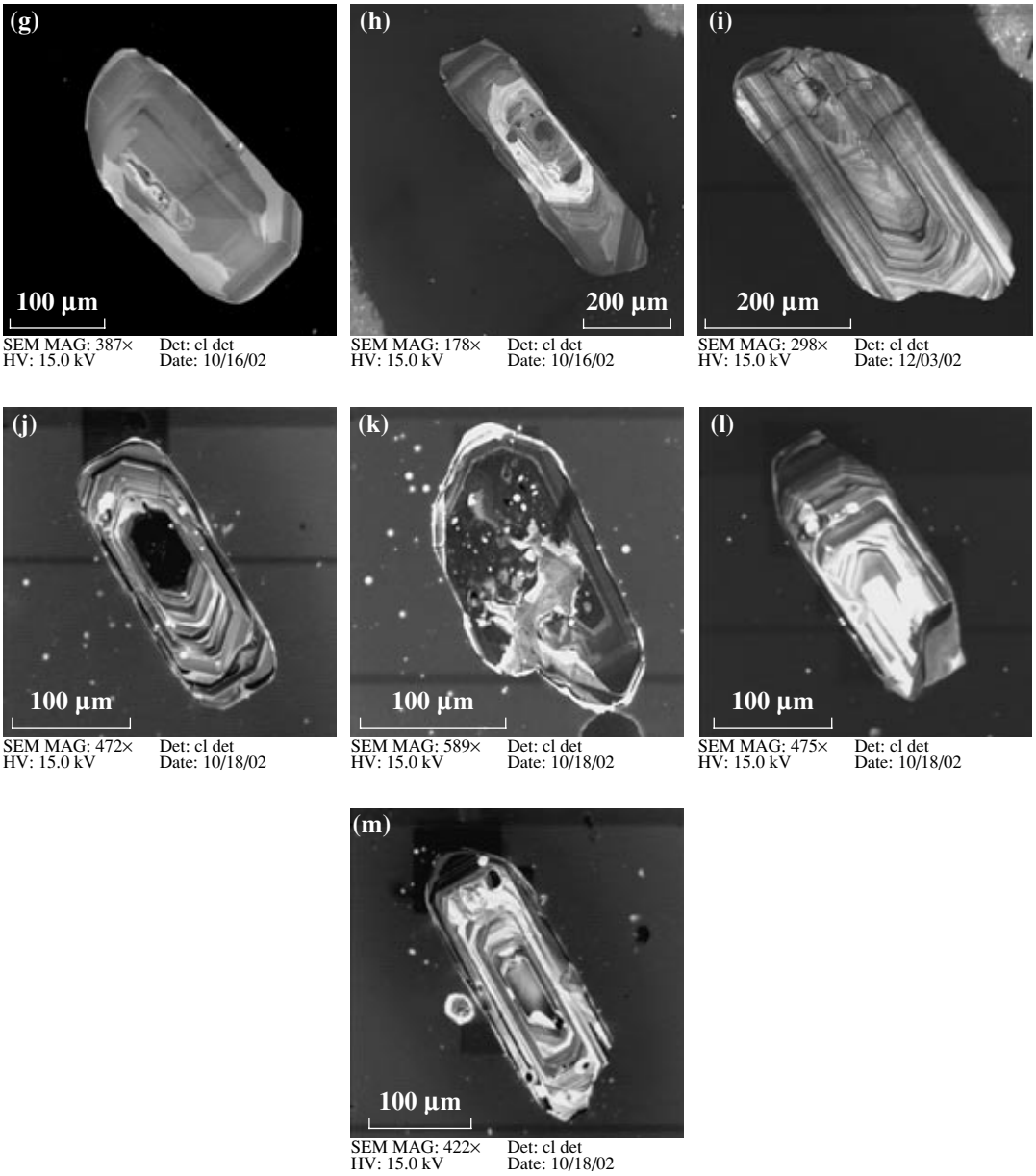

Fig. 6. (Contd.).

using CLC (Table 3, Fig. 6i, no. 7) has, conversely, the youngest $^{207}Pb/^{206}Pb$ age, and its isotopic composition point plots to the left of the discordia, perhaps, because of the incomplete removal of its recrystallized parts (paler zones in the outer portion of the grain) during its air abrasion. Obviously, the acid treatment of the zircon at various exposures resulted in the removal of various disturbed phases (relics of ancient cores, recrystallized fragments of seemingly younger age, and grain portions affected by the modern loss of radiogenic lead). With regard for these considerations, the most accurate estimate of the crystallization age of the Dzheluiskii enderbite seems to be the date corresponding to the upper intercept of the discordia: 2627 ± 16 Ma.

Accessory zircon from the charnockite from the Altual'skii Complex comprises turbid and transparent subhedral prismatic grains of brownish cherry and pale pink color. The zircon crystals are faceted with {100} and {110} prisms and {101}, {111}, and {201} dipyramids, and their sizes range from 30 to 350 μm at K_{elong} = 2.2–6.0. The zircon sample was provisionally subdivided into three types of zircon grains based on their habits, which, in fact, differ from one another only by the degrees of high-temperature recrystallization. Type I (50%) comprises turbid, extensively fractured subhedral zircon crystals of prismatic habit (Fig. 6d) and brownish cherry color. They are characterized by thin zoning and the presence of thin outer rims with strong cathodoluminescence. The same grains possibly have

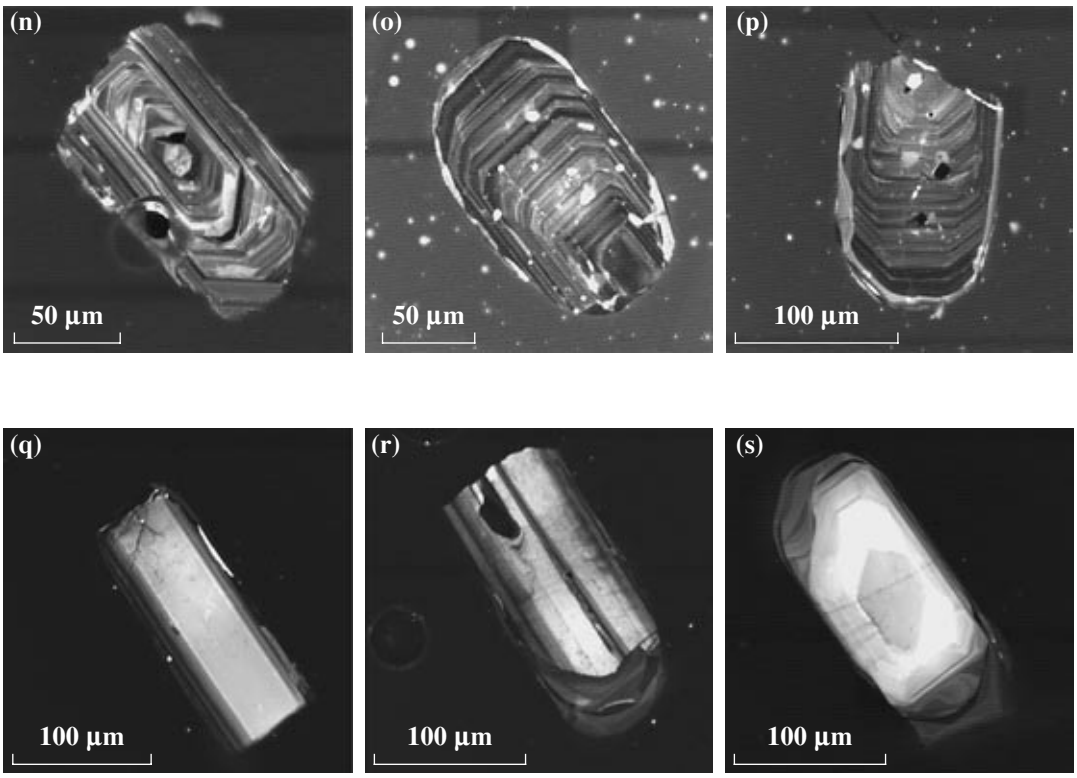

Fig. 6. (Contd.).

metamict cores (Figs. 6j, 6k). The type-II zircon (30%) consists of semitransparent or, more rarely, transparent subhedral crystals of brownish cherry color and long-prismatic zircon habit (Fig. 6e). Similarly to the type-I zircon, this modification of the mineral is zonal, but its grains have more extensive recrystallized portions with bright CL (Figs. 6l, 6m). Type III (20%) consists of subhedral transparent zircon crystals of pale pink color and prismatic or long-prismatic morphology (Fig. 6f). As can be seen in Figs. 6q–6s, the type-III zircon differs from the type-I and type-II zircons in having stronger luminescence and virtually no primary magmatic zoning, which is preserved only in the marginal parts of the crystals. This is most probably explained by the high-temperature recrystallization of this mineral.

The U–Pb isotopic study was initially conducted with relatively large samples (up to 0.8 mg) of all of the types recognized (Table 3, nos. 8–14), with some zircon samples (Table 3, nos. 12–14) subjected to air abrasion. Dates were then obtained for single zircon grains, which have been preliminarily examined by CLC. This enabled us to analyze zircon crystals that were least weakly affected by secondary alterations. The isotopic composition points of zircon of type I from the size fraction +100–150 μm, of zircon of types I and III after air abrasion, and the isotopic composition point of three fragments of zircon grains with insignificant discordance (2%) define a discordia whose upper intercept with the concordia corresponds to an age of 2612 ± 6 Ma, and the lower intercept corresponds to 757 ± 110 Ma (MSWD = 1.4). The isotopic composition points of the type-II zircon from the size fraction +100–150 μm (Table 3, no. 9) and the untreated zircon of type III (Table 3, nos. 10. 11) plot to the left of the discordia. The type-III zircon has a much younger $^{207}Pb/^{206}Pb$ age (<2500 Ma). The type-II zircon after air abrasion (Table 3, no. 12) has a slightly older age (2624 ± 0.6 Ma), perhaps, because of the presence of a fraction containing an ancient inherited component of radiogenic Pb.

With regard for the aforesaid, the most accurate dating of the charnockite age should be taken equal to 2612 ± 6 Ma, which was yielded by the upper intercept of the discordia. The high-temperature recrystallization of type-II and III zircons was likely related to the early Proterozoic metamorphic event, which widely affected the Aldan Shield and Dzhugdzhur–Stanovoi foldbelt.

ISOTOPIC GEOCHEMISTRY

Sm–Nd isotopic systematics. The results of the Sm–Nd isotopic studies of the mafic rocks and charnockites of the Kalar Complex and their host enderbites of the Dzheluiskii Complex, charnockites of the Altual'skii Complex, and gneisses of the Kurulta Formation are summarized in Table 4 and portrayed in Fig. 8.

The broadest variations in the values of ε_{Nd} and the Nd model ages are typical of the anorthosites [$\varepsilon_{Nd}(T)$ from –5.4 to +0.5, $T_{Nd}(DM)$ = 3.4–2.9 Ga], whereas the

Table 3. U–Pb isotopic data on zircon from enderbites of the Dzheluiskii Complex and charnockites of the Altual'skii Complex

no.	Size fraction (μm) and its characteristics	Sample (mg)	Concentration (ppm)		Isotopic ratios					Rho	Age (Ma)		
			Pb	U	$^{206}Pb/^{204}Pb$	$^{207}Pb/^{206}Pb^{a}$	$^{208}Pb/^{206}Pb^{a}$	$^{207}Pb/^{235}U$	$^{206}Pb/^{238}U$		$^{207}Pb/^{235}U$	$^{206}Pb/^{238}U$	$^{207}Pb/^{206}Pb$
Enderbite, Dzheluiskii Complex (sample 3713)													
1	+70–80	0.61	56.3	114	9062	0.1620 ± 1	0.1754 ± 1	9.611 ± 19	0.4304 ± 8	0.93	2398 ± 5	2308 ± 5	2476 ± 0.7
2	>150	1.07	46.5	94.9	7843	0.1590 ± 1	0.1717 ± 1	9.443 ± 19	0.4308 ± 8	0.91	2382 ± 5	2309 ± 5	2445 ± 0.7
3	>150, A 50%, 10 grains	–	U/Pb* = 1.76		2664	0.1748 ± 1	0.1875 ± 1	11.697 ± 23	0.4852 ± 10	0.93	2581 ± 5	2550 ± 5	2604 ± 0.9
4	>150, A 70%, 5 grains	–	U/Pb* = 1.67		652	0.1764 ± 1	0.2120 ± 1	11.648 ± 27	0.4790 ± 11	0.95	2577 ± 6	2523 ± 6	2619 ± 1.2
5	>150, IR 4 h	–	U/Pb* = 1.85		11011	0.1692 ± 1	0.1769 ± 1	10.907 ± 22	0.4676 ± 9	0.97	2515 ± 5	2473 ± 5	2550 ± 0.6
6	>150, IR 6 h	–	U/Pb* = 1.73		1008	0.1716 ± 1	0.1854 ± 1	11.345 ± 23	0.4794 ± 10	0.92	2552 ± 5	2525 ± 5	2574 ± 0.9
7	>150, A 40%, CLC, single grain	–	U/Pb* = 1.96		551	0.1509 ± 3	0.2531 ± 2	8.599 ± 45	0.4132 ± 19	0.95	2296 ± 12	2230 ± 10	2356 ± 3.0
Charnockite, Altual'skii Complex (sample 3796-1)													
8	I, +100–150	0.41	326	620	4186	0.1727 ± 1	0.1510 ± 1	10.972 ± 22	0.4609 ± 9	0.93	2521 ± 5	2443 ± 5	2584 ± 0.6
9	II, +100–150	0.65	74.3	135	5576	0.1718 ± 1	0.1734 ± 1	11.262 ± 23	0.4753 ± 10	0.91	2545 ± 5	2507 ± 5	2576 ± 0.8
10	III, +100–150	0.63	68.9	140	3943	0.1615 ± 1	0.1342 ± 1	9.818 ± 20	0.4411 ± 9	0.90	2418 ± 5	2355 ± 5	2471 ± 0.8
11	III, +80–60	0.54	87.2	182	7442	0.1640 ± 1	0.1403 ± 1	9.6932 ± 19	0.4286 ± 9	0.87	2406 ± 5	2299 ± 5	2498 ± 1.1
12	II, +100–150, A 20%	0.35	235	398	18875	0.1768 ± 1	0.2271 ± 1	12.029 ± 24	0.4933 ± 10	0.93	2607 ± 5	2585 ± 5	2624 ± 0.6
13	I, +100–150, A 10%	0.41	445	813	16475	0.1741 ± 1	0.1590 ± 1	11.513 ± 23	0.4795 ± 10	0.94	2566 ± 5	2525 ± 5	2598 ± 0.6
14	III, +100–150, A 30%	0.88	25.9	50.9	3712	0.1701 ± 3	0.1874 ± 1	10.236 ± 27	0.4364 ± 9	0.81	2456 ± 6	2335 ± 5	2559 ± 2.5
15	I, <100, A 20%, CLC, 3 single grains	–	U/Pb* = 1.71		187	0.1739 ± 5	0.2039 ± 1	11.569 ± 159	0.4827 ± 64	0.98	2570 ± 35	2539 ± 34	2595 ± 5.0

Note: [a] Isotopic ratios are corrected for the blank and common Pb; I, II, and III are the morphological types of zircon; A 50% is the amount of material removed during zircon air abrasion; IR – insoluble residue after acid treatment. CLC corresponds to cathodoluminescence monitoring. The errors (2σ) correspond to two significant decimal digits; * zircon sample was not determined.

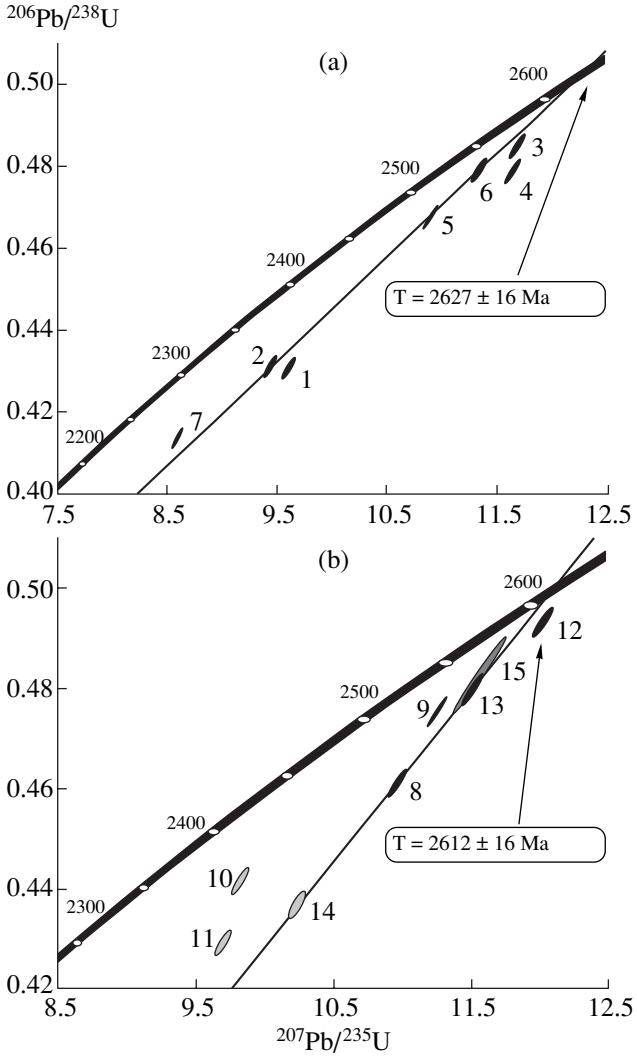

Fig. 7. Concordia diagram for zircon from (a) enderbite of the Dzheluiskii Complex (sample 3713) and (b) charnockite of the Altual'skii Complex (sample 3796-1).

charnockites of the Kalar Complex show much narrower variations of these parameters [$\varepsilon_{Nd}(T)$ from –2.4 to –1.0, $T_{Nd}(DM)$ = 3.1–3.0 Ga]. The enderbites of the Dzheluiskii Complex and the charnockites of the Altual'skii Complex have Nd isotopic characteristics closely similar to those of the Kalar charnockites [$\varepsilon_{Nd}(T)$ from –2.7 to –1.0, $T_{Nd}(DM)$ = 3.1–3.0 Ga].

The $\varepsilon_{Nd}(T)$ age diagram in Fig. 8 displays the isotopic data points of rocks of the Kalar Complex, enderbites of the Dzheluiskii Complex, charnockites of the Altual'skii Complex, the isotopic evolution field of the Archean continental crust of the Chara–Olekma geoblock in the Aldan Shield, and the isotopic evolution lines of gneisses from the Kurulta block. As follows from this diagram, the Kurulta gneisses bear slightly more radiogenic Nd than that in the rocks of the Chara–Olekma geoblock and have younger Nd model ages: 3.0–2.8 and 3.7–2.9 Ga, respectively. The Nd isotopic composition points of the Kalar charnockites, the Dzheluiskii enderbites, and the Altual'skii charnockites define a fairly compact field in the upper part of the Nd isotopic evolution field for the continental crust of the Chara–Olekma geoblock (Olekma granite–greenstone terrane).

Pb–Pb isotopic systematics. The most distinctive feature of the isotopic data obtained on both the acid leachates and residues after leaching plagioclase from the Kalar anorthosites (Table 5, Fig. 9) is the significant variations in the measured ratios and a notably more radiogenic Pb isotopic composition than that of the model common Pb of Late Archean rocks and ores (Stacey and Kramers, 1975). Residues after feldspar acid leaching usually have low U/Pb ratios, and their Pb isotopic composition can be used to evaluate the initial Pb isotopic composition of the unmetamorphosed rocks (Doe, 1970; Ludwig and Silver, 1977).

There can be two reasons for the significant deviations of the measured isotopic ratios from the model values of the samples: (i) the occurrence of syngenetic coeval inclusions with a high U/Pb ratio in the feldspar and (ii) Pb redistribution between this feldspar and a rock with a high U/Pb ratio during a younger overprinted process, which resulted in a "freezing" of the Pb isotopic composition of the feldspar that was averaged at the time of the overprinted process. The latter explanation seems to be more plausible, because the feldspar fractions were hand-picked very carefully. In this situation, the line defined by pairs of the leachate–residue data points in a $^{206}Pb/^{204}Pb$–$^{207}Pb/^{204}Pb$ diagram should have a slope corresponding to the apparent age values that should be younger than the actual age of the rocks (Neymark *et al.*, 1998).

Our Pb isotopic data on plagioclase define three leachate–residue trends (Fig. 9), whose slopes correspond to ages of 2420 ± 120, 2158 ± 210, and 2105 ± 220 Ma. With regard for the aforesaid, these estimates are likely some intermediate values between the actual age of these rocks and the age of an overprinted process. The Pb isotopic data on the plagioclase residues after leaching define a single linear regression (MSWD = 0.46), which is a so-called T_1–T_2 isochron. The parameters of this isochron can be used to date the overprinted process (T_2) upon specifying the age of the magmatic rock (T_1). For T_1 = 2.6 Ga (the U–Pb crystallization age of anorthosites in the Kalar Complex), we obtain T_2 of about 1.9 Ga, which is generally consistent with the U–Pb zircon age of the overprinted high-grade metamorphic event (1.85 Ga; Sal'nikova *et al.*, 2004a). The value of μ_2 ($^{238}U/^{204}Pb$) = 9.2–9.3 in the source of the anorthosites [according to the model (Stacey and Kramers, 1975)] and the location of the Pb isotopic composition points of the anorthosites close to the evolutionary trajectory of the Pb isotopic composition of the lower continental crust in a $^{206}Pb/^{204}Pb$–$^{207}Pb/^{204}Pb$ diagram (Fig. 9, plumbotectonics-2 model; Zartman and Doe, 1981) suggest that the parental magma of the

Table 4. Sm–Nd isotopic data on magmatic rocks from the Kalar Complex and the host granitoids and gneisses

Sample	Rock	Age, Ma	Sm, ppm	Nd, ppm	$^{147}Sm/^{144}Nd$	$^{143}Nd/^{144}Nd \pm 2\sigma$	$\varepsilon_{Nd}(T)$	$T_{Nd}(DM)$-1st, Ma	$T_{Nd}(DM)$-2st, Ma
Imangakit Massif									
A-80-1*	anorthosite	2620	1.118	5.48	0.1233	0.511336 ± 24	–0.6	3026	
K-81-4*	gabbroanorthosite	2620	0.334	1.832	0.1103	0.511172 ± 22	0.5	2890	
T-3*	anorthosite	2620	0.1661	0.924	0.1087	0.510843 ± 22	–5.4	3314	
1279*	charnockite	2620	5.83	31.2	0.1132	0.511073 ± 23	–2.4	3117	3153
Kuronaakh Massif									
T-1*	gabbroanorthosite	2620	13.06	68.8	0.1148	0.511167 ± 23	–1.1	3026	
KA-12	anorthosite	2620	0.310	1.98	0.0962	0.510867 ± 22	–0.7	2935	
KA-13	anorthosite	2620	0.74	4.18	0.1075	0.511118 ± 8	0.5	2890	
KA-4	metagabbro	2620	1.070	5.37	0.1205	0.511266 ± 7	–1.1	3050	
1267*	charnockite	2620	14.78	77.6	0.1152	0.511177 ± 23	–1.0	3024	3044
Dzheluiskii Massif									
3706	enderbite	2630	2.37	17.38	0.0823	0.510542 ± 6	–2.2	3009	3161
3713	enderbite	2630	7.37	42.5	0.1047	0.510989 ± 5	–1.0	3006	3067
Altual'skii Massif									
3905	charnockite	2630	7.17	46.9	0.0924	0.510709 ± 5	–2.3	3050	3174
3796-1	charnockite	2630	12.82	73.2	0.1058	0.510921 ± 5	–2.8	3132	3208
Kurulta Formation									
3-87	gneiss		4.00	24.4	0.0990	0.510903 ± 23	–0.9	2959	
7-87	gneiss		3.70	19.65	0.1140	0.511154 ± 22	–1.0	3020	
16-87	gneiss		1.232	10.48	0.0711	0.510480 ± 22	0.3	2830	
19-87	gneiss		1.839	12.86	0.0864	0.510692 ± 23	–0.8	2918	

Note: The values of ε_{Nd} for the gneisses of the Kurulta Formation are recalculated for the age of the Kalar Complex (2620 Ma).
* Analytical data are from (Sukhanov and Zhuravlev, 2002).

anorthosites was derived by the melting of a lower crustal source, or the parental magma was of mantle provenance but was significantly contaminated by the material of the Archean lower crust.

DISCUSSION

The previously obtained U–Pb zircon ages of various rocks that form the Kuronaakh Massif of the Kalar Complex (augite–hypersthene charnockite, hypersthene–hornblende metagabbro from the marginal melanocratic complex, and hypersthene-bearing anorthosite) demonstrate that all of them were formed within a fairly narrow time span, 2623 ± 23 Ma (Sal'nikova *et al.*, 2004a), which testifies to the syngenetic character of these rocks, i.e., their affiliation with a single magmatic association. Geological, mineralogical, and geochemical characteristics of the Kalar anorthosites are practically identical to the aforementioned indicator features of massif-type anorthosites (Ashwal, 1993; Wiebe, 1992). The only difference of our rocks from classic anorthosites of this type is their age. As was mentioned above, the extensive formation of the latter rocks was related mostly to the Mesoproterozoic geologic epoch, whereas the Kalar anorthosites have a Late Archean age.

The charnockites of the Kalar Complex are typical reduced rapakivi-type granitoids, which affiliate with the ilmenite metaluminous series of A-granites (Frost and Frost, 1997). There are good reasons to believe that the Kalar Complex belongs to the AMCG association and is the oldest of all of its known examples. The composition and geologic setting of this complex are the closest to those of Neoproterozoic anorthosite–charnockite plutons of the Grenville Province and the Rogoland Massif in Norway.

The Altual'skii charnockites, which are ascribed to the Kalar Complex by several geologists (Priyatkina and Lavrovich, 1985; Levchenkov *et al.*, 1987) principally differ from the charnockites of this complex. The geologic features of the Altual'skii charnockites make them similar to the Dzheluiskii enderbites, which are typical synmetamorphic granitoids (Shemyakin and Kotov, 1985; Kotov and Samorukova, 1990) and sometimes show geochemical characteristics of Archean rocks belonging to the TTG association.

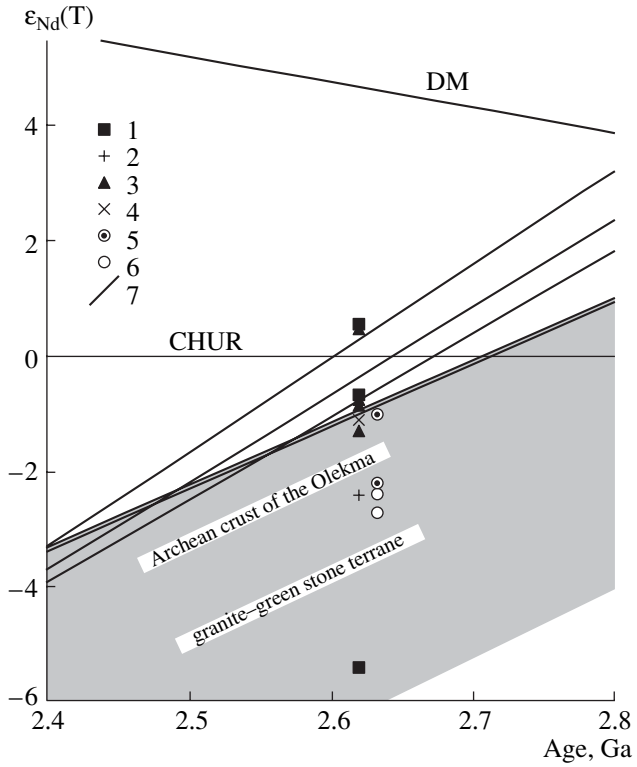

Fig. 8. Diagram $\varepsilon_{Nd}(T)$ –age for rocks of the Kalar Complex and host rocks.

(1–4) Kalar Complex: (1, 2) Imangakit Massif: (1) mafic rocks, (2) charnockites; (3, 4) Kuronaakh Massif: (3) mafic rocks, (4) charnockites; (5, 6) synmetamorphic granitoids: (5) enderbites of the Dzheluiskii Complex, (6) charnockites of the Altual'skii Complex; (7) evolutionary trajectory for the Nd isotopic composition of gneisses of the Kurulta Formation. The diagram shows the evolutionary lines of the undifferentiated Earth (CHUR) and depleted mantle (DM) (Goldstein and Jacobsen, 1988) and the evolutionary field of the Archean crust of the Chara–Olekma geoblock (Sal'nikova *et al.*, 1996).

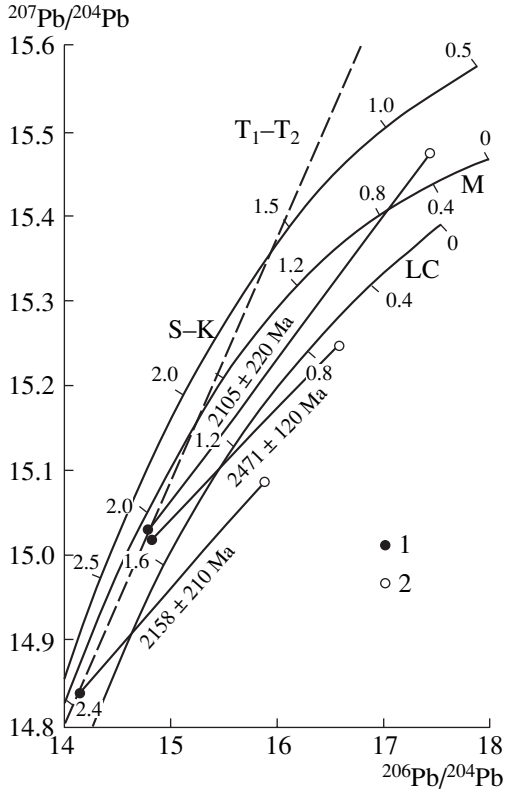

Fig. 9. $^{207}Pb/^{204}Pb$ vs $^{206}Pb/^{204}Pb$ diagram for plagioclase from mafic rocks of the Kalar Complex.

(1) Acid-leached residues; (2) acid leachates. Evolutionary trajectories of the Pb isotopic composition: S–K—model trajectory from (Stacey and Kramers, 1975), LC and M—lower crustal and mantle trajectories, respectively (plumbotectonics model, Zartman and Doe, 1981). Numerals near lines correspond to model ages (Ga). Numerals near two-point (leachate–residue) Pb–Pb isochrons are the apparent ages (Ma) estimated from the slopes of the lines. T_1–T_2 is the Pb–Pb isochron based on the acid-leached residues of plagioclase (MSWD = 0.46).

The aforementioned U–Pb zircon dates of the Dzheluiskii enderbites and Altual'skii charnockites indicate that their ages are closely similar: 2627 ± 16 and 2612 ± 6 Ma, respectively. The emplacement of these massifs was related to the third episode of granulite metamorphism in the Kurulta block (Sal'nikova *et al.*, 2004b).

The age of granitoids from the Dzheluiskii and Altual'skii complexes corresponds, within the errors, to the age of the rocks from the Kalar Complex. At the same time, geological evidence indicates that the age of the former rocks should be older. This implies that the massifs of the Kalar Complex were emplaced immediately before the granulite metamorphism that was associated with the origin of the charnockite–enderbite plutons.

Judging from Nd isotopic data (Table 4, Fig. 8), the Dzheluiskii enderbites and Altual'skii charnockites were produced by the melting of the continental crust, predominantly that of the Chara–Olekma geoblock. The enderbites are geochemically close to the TTG association and differ from the charnockites in having a slightly more radiogenic Nd isotopic composition. Enderbites of this type can be formed by the following magma-generating processes: (i) the partial melting of eclogite or garnet-bearing mafic granulite (Arth and Hanson, 1972; Compton, 1978) or (ii) the partial melting of basaltic rocks that had been metamorphosed to the amphibolite facies (Condie, 1986; Martin, 1994). The fairly wide occurrence of mafic garnet-bearing crystalline schists among the rocks of the Kurulta block indicates that these rocks can highly probably be produced by the partial melting of mafic garnet-bearing rocks. The extremely strongly fractionated character of the REE patterns of the enderbite [$(La/Yb)_N$ = 42.5), their low HREE concentrations [$(Yb)_N$ = 1.48], and the concave configuration of the REE patterns over HREE (Fig. 7) were most probably caused by the presence of hornblende and garnet in the residue (Martin, 1994). The clearly pronounced Ta–Nb anomaly also testifies

that the residue contained hornblende (Drummond and Defant, 1990). The somewhat less radiogenic Nd isotopic composition of the charnockites suggests that these rocks were derived by the melting of a source with a higher proportion of the material of the ancient sialic crust.

The similarities between the isotopic compositions of the charnockites from the Kalar Complex, the enderbites from the Dzheluiskii Complex, and the charnockites from the Altual'skii Complex provide evidence that all of these rocks were derived from the same sources, and the Kalar charnockites are of predominantly crustal nature. The geochemical differences between these rocks were most probably caused by the different depths and conditions of magma-generation and also by the further evolution of the parental magmas. Granulite metamorphism is known to be associated with ultrametamorphic processes, during which large volumes of granite material are mobilized, and this results in the origin of residual granulites. Some researchers (Collins *et al.*, 1982; Clemens *et al.*, 1986) believe that these granulites could be the possible source material of granites of type A, to which the Kalar charnockites also affiliate. The low degrees of the partial anhydrous melting of such a source within the lower crust produces the parental magmas of granites of this type. In the absence of water, melting under the effect of a mantle thermal source is initiated by the decomposition of F-rich H_2O-bearing mafic silicates (Clemens *et al.*, 1986).

The significantly less radiogenic Nd compositions of the enderbites and charnockites of the Dzheluiskii and Altual'skii complexes compared with those of the host gneisses of the Kurulta Formation suggest that the latter could not serve as the crustal source material of the former. This means that the Kurulta block is most probably a tectonic slab of relatively low thickness, which was thrust over the southern flank of the Chara–Olekma geoblock during the Late Archean collisional event.

The broad variations in the initial ε_{Nd} values of the Kalar mafic rocks (Table 4, Fig. 8) testify that their source was enriched, perhaps, because of the assimilation of the host rocks in the chamber, contamination before the emplacement of the melt, the derivation of the magma from an enriched mantle source, or a combination of these mechanisms. Isotopic and geochemical data on the anorthosites, typical Proterozoic members of the AMCG association (Piercey and Wilton, 1999; Emslie *et al.*, 1994; Stein *et al.*, 1998; Larin *et al.*, 2002) indicate that their parental mantle magma could dissolve up to 75% continental crustal material. Because of this, the Nd isotopic characteristics of the anorthosites often reflect not the composition of the mantle source but the compositions of the crustal contaminants or are intermediate between the characteristics of the sources and crustal contaminants (Larin *et al.*, 2002). The parental magma of the anorthosites, whose Nd concentration was more than one order of magnitude lower than that in the associated charnockites (Table 4), was isotopically much more sensitive to crustal contamination. Because of this, the variations in the $\varepsilon_{Nd}(T)$ of the anorthosites likely provide evidence of such processes. However, the absence of correlations between the Nd isotopic composition and some geochemical parameters indicative of crustal contamination (Mg#, Cr, Rb, and Zr) points out that the variations in the $\varepsilon_{Nd}(T)$ were caused not so much by the degree of contamination as by the heterogeneity of the crustal contaminant. With regard for the complicated polybaric character of the crystallization of massif-type anorthosites (Emslie, 1985; Emslie *et al.*, 1994; Ashwal, 1993), the possibility of crustal contamination with rocks of various compositions and ages at different depths seems to be plausible enough (Larin *et al.*, 2002). Pb isotopic data indicate that the contaminant was dominated by lower crustal material. The charnockite magma, whose Nd concentration was much higher than that of the host rocks and, particularly, of the anorthosites, was "isotopically" less sensitive to crustal contamination, and its isotopic signatures reflect mostly the composition of the deep crustal source of these rocks.

Table 5. Pb–Pb isotopic data on plagioclase from anorthosites of the Kalar Complex

Sample	Leachate/residue	Pb isotopic composition		
		$^{206}Pb/^{204}Pb$	$^{207}Pb/^{204}Pb$	$^{208}Pb/^{204}Pb$
3	Residue	14.799	15.019	34.701
	Leachate	16.569	15.250	36.495
K-158	Residue	14.824	15.035	34.840
	Leachate	17.471	15.449	37.503
KA-17	Residue	14.121	14.837	33.905
	Leachate	15.897	15.076	35.498

Note: Analyses were conducted by B.M. Grokhovskii and I.M. Vasil'eva at the Institute of Precambrian Geology and Geochronology (IGGD), Russian Academy of Sciences.

An important problem is the tectonic setting of the AMCG association. Until recently it was traditionally thought to be anorogenic (Anderson, 1983; Rämö and Haapala, 1995). However, newly obtained data indicate that many magmatic complexes of this association have a within-plate setting but are not anorogenic (Larin, 2004; Karlstrom *et al.*, 2001). Modern geologic, geochronologic, geochemical, and isotopic data indicate that the AMCG association can be subdivided into two groups with different tectonic settings (Larin, 2004): (i) anorogenic and (ii) related to orogenic processes. The AMCG association of the latter group can be, in turn, subdivided into two types: (a) related to collisional orogens and (b) related to long-lived (~2.0–1.0 g.y.) peripheral accretionary orogens. The Kalar AMCG association affiliates with the first type of the second group. The metamorphic event at 2.63 Ga, which was

recognized by the authors of this publication (Larin *et al.*, 2004; Sal'nikova *et al.*, 2004b) in the geologic evolution of the Dzhugdzhur–Stanovoi foldbelt and its junction zone with the Aldan Shield, had been reportedly related to the amalgamation and subsequent collision of terranes that now compose the granulite basement of the Dzhugdzhur–Stanovoi foldbelt with the Olekma–Aldan continental plate (Kotov, 2003; Larin *et al.*, 2004). The time gap between this collision event and the emplacement of the massifs of the Kalar Complex did not exceed 30 m.y. In other words, there are good reasons to believe that the Kalar AMCG association was produced in a postcollisional setting. It is also important to mention that the adjacent southwestern part of the Aldan Shield shows traces of a number of roughly coeval pulses of syn- and postcollisional granitoid magmatism (2.68–2.60 Ga; Kotov, 2003).

Possible tectonic analogues of the Kalar Complex are the plutons of the AMCG association (1.16–1.13 and 1.09–1.05 Ga) in the Grenville orogen and the Rogoland Massif (0.93–0.92 Ga) in the Sveconorwegian fold area. These plutons were also emplaced in postcollilsional environments (Corrigan and Hanmer, 1997; Bolle *et al.*, 2003). The genesis of these plutons can be explained within the scope of the model of lithospheric delamination, the collapse and extension of a collisional orogen, and the subsequent emplacement of high-temperature mafic magmas related to a lithospheric source.

The high-grade metamorphic event (~1.9 Ga) that affected the rocks of the Kalar Complex, was related to the docking of the Dzhugdzhur–Stanovoi continental microplate to the Siberian craton (Larin *et al.*, 2002, 2004; Sal'nikova *et al.*, 2004a) as a result of the closure of an oceanic structure in the Early Proterozoic. A probable trace of this structure is the Stanovoi suture zone, which separates the Dzhugdzhur–Stanovoi fold area and Aldan Shield (Gusev and Khain, 1995).

Hence, the Aldan–Stanovoi Shield includes two spatially separated AMCG associations, which have different ages and tectonic settings. The Late Archean postcollisional plutons of the Kalar Complex are localized exclusively within the junction zone of the Aldan Shield and Dzhugdzhur–Stanovoi folded area. The Dzhugdzhur anorthosites and the rocks of the Ulkan Complex compose an Early Proterozoic (1.74–1.70 Ga) AMCG association, which is a component of the Bilyakchan–Ulkan volcano-plutonic belt. The latter extends for more than 750 km from the Mongolia–Okhotsk lineament to the Okhotsk Massif and "glues" the Early Precambrian tectonic structures to the southeastern part of the Siberian Platform (Larin *et al.*, 1997).

CONCLUSIONS

1. The rocks of the Kalar Complex belong to an AMCG magmatic association and are its oldest members. The massifs of the Kalar Complex were produced in a postcollisional environment. The time gap between the collisional event and the emplacement of the massifs of the Kalar Complex was no longer than 30 m.y.

2. The charnockites and anorthosites of the Kalar Complex are a single syngenetic magmatic association. The charnockites have a predominantly crustal nature, whereas the anorthosites were most probably formed by a mantle magma that was significantly crustally contaminated at various depth levels.

3. The southern part of the Siberian Platform includes two reliably identified AMCG associations, which are spatially separated and have distinct ages, compositions, and tectonic settings: (i) the Late Archean (2.62 Ga) postcollisional Kalar plutonic complex and (ii) the Early Proterozoic (1.74–1.70 Ga) anorogenic Ulkan–Dzhugdzhur volcano-plutonic complexes.

ACKNOWLEDGMENTS

The authors thank G.V. Ovchinnikova (Institute of Precambrian Geology and Geochronology (IGGD), Russian Academy of Sciences) for valuable recommendations and comments expressed during the discussion of the manuscript. We also thank G.P. Medvedev and V.I. Beloshapkin, residents of the village of Yuktali, Amur oblast, for altruistic help with the organization and conduction of the fieldwork. This study was financially supported by the Russian Foundation for Basic Research (project nos. 00-05-72011, 02-05-64209, 02-05-65086, 03-05-64893, and 04-05-64810), a grant for a research school (Grant NSh-615.2003.05), the programs for fundamental research "Geodynamic Evolution of the Lithosphere in the Central Asian Foldbelt: From a Paleocean to a Continent" and "Isotopic Geology: Geochronology and Material Sources" of Earth Science Division, Russian Academy of Sciences, and the Foundation for Sponsoring the National Science.

REFERENCES

1. J. L. Anderson, "Proterozoic Anorogenic Granite Plutonism of North America," in *Proterozoic Geology: Selected Papers from an International Proterozoic Symposium*, Ed. by L. G. Medaris, C. W. Byers, D. M. Mickelson, and W. C. Shnaks, Geol. Soc. Am. Mem. **161**, 133–154 (1983).
2. J. G. Arth and G. N. Hanson, "Quartz Diorites Derived by Partial Melting of Eclogite Or Amphibolite at Mantle Depths," Contrib. Mineral. Petrol. **37**, 161–174 (1972).
3. L. D. Ashwal, *Anorthosites, Minerals and Rocks* (Springer, Berlin, 1993).
4. G. N. Bazhenova, "Anorthosites of the Kalar Pluton," in *Anorthosites of the USSR*, Ed. by O. A. Bogatikov (Nauka, Moscow, 1974), pp. 85–99 [in Russian].
5. O. A. Bogatikov, *Anorthosites* (Nauka, Moscow, 1979) [in Russian].
6. O. Bolle, D. Demaiffe, and J.-C. Duchesne, "Petrogenesis of Jotunitic and Acidic Members of an AMC Suite (Rogoland Anorthosite Province, SW Norway): A Sr and

Nd Isotopic Assessment," Precambrian Res. **124**, 185–214 (2003).

7. J. D. Clemens, J. R. Holloway, and A. J. R. White, "Origin of an A-Type Granite: Experimental Constraints," Am. Mineral. **71**, 317–324 (1986).
8. W. J. Collins, S. D. Beams, A. J. R. White, and B. W. Chappell, "Nature and Origin of A-Type Granites with Particular Reference to Southeastern Australia," Contrib. Mineral. Petrol. **80**, 189–200 (1982).
9. P. Compton, "Rare Earth Element Evidence for the Origin of the Nûk Gneisses, Buksefjorden Region, Southern West Greenland," Contrib. Mineral. Petrol. **66**, 283–294 (1978).
10. K. C. Condie, "Chemical Composition and Evolution of the Upper Continental Crust: Contrasting Results from Surface Samples and Shales," Chem. Geol. **104**, 1–37 (1993).
11. K. C. Condie, "Origin and Early Growth Rate of Continents," Precambrian Res. **32**, 261–278 (1986).
12. D. Corrigan and S. Hanmer, "Anorthosites and Related Granitoids in the Grenville Orogen: A Product of Convective Thinning of the Lithosphere," Geology **25**, 61–64 (1997).
13. B. R. Doe, *Lead Isotopes* (Springer, Berlin, 1970).
14. M. S. Drummond and M. J. Defant, "A Model for Trondhjemite–Tonalite–Dacite Genesis and Crustal Growth via Slab Melting: Archean to Modern Comparisons," J. Geophys. Res. **95** (B13), 503–521 (1990).
15. R. F. Emslie and P. A. Hunt, "Ages and Petrogenetic Significance of Igneous Mangerite–Charnockite Suites Associated with Massif Anorthosites, Grenville Province," J. Geol. **98**, 213–231 (1990).
16. R. F. Emslie, "Proterozoic Anorthosite Massifs," in *The Deep Proterozoic Crust in the North Atlantic Provinces*, Ed. by A. Tobi and J. L. R. Touret (Reidel, Dordrecht, 1985), pp. 39–60.
17. R. F. Emslie, M. A. Hamilton, and R. J. Theriault, "Petrogenesis of a Mid-Proterozoic Anorthosite–Mangerite–Charnockite–Granite (AMCG) Complex: Isotopic and Chemical Evidence from the Nain Plutonic Suite," J. Geol. **102** (5), 539–558 (1994).
18. C. D. Frost and B. R. Frost, "Reduced Rapakivi-Type Granites: The Tholeiite Connection," Geology **25**, 647–650 (1997).
19. S. J. Goldstein and S. B. Jacobsen, "Nd and Sr Isotopic Systematics of River Water Suspended Material: Implications for Crustal Evolution," Earth Planet. Sci. Lett. **87** (3), 249–265 (1988).
20. G. S. Gusev and V. E. Khain, "Relations between Baikal–Vitim, Aldan–Stanovik, and Mongolia–Okhotsk Terrains," Geotektonika, No. 5, 68–82 (1995).
21. M. D. Higgins and O. van Breemen, "Three Generations of Anorthosite–Mangerite–Charnockite–Granite (AMCG) Magmatism, Contact Metamorphism, and Tectonism in the Saguenay–Lac–Saint-Jean Region of the Grenville Province, Canada," Precambrian Res. **79**, 327–346 (1996).
22. S. B. Jacobsen and G. J. Wasserburg, "Sm–Nd Evolution of Chondrites and Achondrites," Earth Planet. Sci. Lett. **67**, 137–150 (1984).
23. K. E. Karlstrom, K.-I. Åhäll, S. S. Harlan, *et al.*, "Long-lived (1.8–1.0 Ga) Convergent Orogen in Southern Laurentia, Its Extensions to Australia and Baltica, and Implications for Refining Rodinia," Precambrian Res. **111**, 5–30 (2001).
24. A. B. Kotov and L. M. Samorukova, *Evolution of Granite Formation in Early Precambrian Tectonic–Metamorphic Cycles* (Nauka, Leningrad, 1990) [in Russian].
25. A. B. Kotov, Extended Abstract of Doctoral Dissertation in Geology and Mineralogy (IGGD RAN, St. Petersburg, 2003).
26. T. E. Krogh, "A Low-Contamination Method for Hydrothermal Decomposition of Zircon and Extraction of U and Pb for Isotopic Age Determination," Geochim. Cosmochim. Acta **37**, 485–494 (1973).
27. T. E. Krogh, "Improved Accuracy of U–Pb Zircon Method by the Creation of More Concordant Systems Using an Air Abrasion Technique," Geochim. Cosmochim. Acta **46**, 637–649 (1982).
28. A. M. Larin, "Types and Tectonic Setting of Rapakivi-Bearing Magmatic Associations," in *Proceedings of the International Conference "The Geology and Metallogeny of Basic–Ultrabasic and Granitoid Intrusive Associations in Folded Belts"* (Yekaterinburg, 2004), pp. 351–354 [in Russian].
29. A. M. Larin, E. B. Sal'nikova, A. B. Kotov, *et al.*, "Late Archean Granitoids of the Dambukinskii Block of the Dzhugdzhur–Stanovik Fold Belt: Formation and Transformation of the Continental Crust in the Early Precambrian," Petrologiya **12** (3), 1–19 (2004) [Petrology **12** (3), 211–226 (2004)].
30. A. M. Larin, V. A. Glebovitsky, R. Sh. Krymsky, and M. K. Sukhanov, "Neodymium and Strontium Isotope Constraints on Genesis of the Geran Anorthosite Massif, Eastern Aldan–Stanovik Shield," Dokl. Akad. Nauk **382** (1), 101–105 (2002) [Dokl. Earth Sci. **382** (1), 35–39 (2002)].
31. A. M. Larin, Yu. V. Amelin, and L. A. Neymark, and R. Sh. Krymsky, "The Origin of the 1.73–1.70 Ga Anorogenic Ulkan Volcano–Plutonic Complex, Siberian Platform, Russia: Inferences from Geochronological, Geochemical and Nd–Sr–Pb Isotopic Data," An. Acad. Bras. Ci **69** (3), 295–312 (1997).
32. A. M. Lennikov, *The Anorthosites of the Southern Aldan Shield and Its Folded Frame* (Nauka, Moscow, 1979) [in Russian].
33. O. A. Levchenkov, I. M. Morozova, G. M. Drugova, *et al.*, "U–Pb Dating of the Oldest Rocks of the Aldan Shield," in *Isotopic Dating of Metamorphism and Metasomatism,* Ed. by Yu. A. Shukolyukov (Nauka, Moscow, 1987), pp. 116–138 [in Russian].
34. T. C. Liew and A. W. Hofmann, "Precambrian Crustal Components, Plutonic Associations, and Plate Environment of the Hercynian Fold Belt of Central Europe: Indications from Nd and Sr Isotopic Study," Contrib. Mineral. Petrol. **98**, 129–138 (1988).
35. K. R. Ludwig and L. T. Silver, "Lead Isotope Unhomogeneity in Precambrian Igneous Feldspars," Geochim. Cosmochim. Acta **41**, 1457–1472 (1977).
36. K. R. Ludwig, "PbDat for MS-DOS, Version 1.21," US Geol. Surv. Open-File Rept., 88-542 (1991).

37. K. R. Ludwig, "ISOPLOT/Ex. Version 2.06: A Geochronological Toolkit for Microsoft Excel," Berkley Geochronol. Center Spec. Publ., No. 1a (1999).
38. *Magmatic Rocks* (Nauka, Moscow, 1985), Vol. 3: *Basic Rocks* [in Russian].
39. H. Martin, "The Archean Grey Gneisses and the Genesis of the Continental Crust," in *Development in Precambrian Geology*, Ed. by K. C. Condie (Elsevier, Amsterdam, 1994), Vol. 11, pp. 205–259.
40. J. M. Mattinson, "A Study of Complex Discordance in Zircons Using Step-wise Dissolution Techniques," Contrib. Mineral. Petrol. **116**, 117–129 (1994).
41. V. N. Moshkin and I. N. Dagelaiskaya, "The Anorthosite Association of the Stanovik and Dhugdzhur Ranges," in *Magmatic Rock Associations* (Nauka, Moscow, 1964), pp. 127–130 [in Russian].
42. L. A. Neymark, A. M. Larin, A. A. Nemchin, *et al.*, "Anorogenic Nature of Magmatism in the Northern Baikal Volcanic Belt: Evidence from Geochemical, Geochronological (U–Pb), and Isotopic (Pb, Nd) Data," Petrologiya **6** (2), 139–164 (1998) [Petrology **6** (2), 124–148 (1998)].
43. L. A. Neymark, A. M. Larin, G. V. Ovchinnikova, and S. Z. Yakovleva, "U–Pb Age of the Dzhugdzhur Anorthosites," Dokl. Akad. Nauk **323** (3), 514–518 (1992).
44. L. A. Neymark, V. P. Kovach, A. A. Nemchin, *et al.*, "Late Archean Intrusive Complexes in the Olekma Granite–Greenstone Terrain (Eastern Siberia): Geochemical and Isotopic Study," Precambrian Res. **62** (4), 453–472 (1993).
45. J. A. Pearce, N. B. W. Harris, and A. G. Tindle, "Trace Element Distribution Diagrams for the Tectonic Interpretation of Granitic Rocks," J. Petrol. **25**, Part 4, 956–983 (1984).
46. S. J. Piercey and D. H. C. Wilton, "Geochemical and Radiogenic Isotope (Sr–Nd) Characteristics of Paleoproterozoic Anorthositic and Granitoid Rocks in Umiakoviarusek Lake Region, Labrador, Canada," Can. J. Earth Sci. **36**, 1957–1972 (1999).
47. U. Poller, V. Liebetrau, and W. Todt, "U–Pb Single Zircon Dating under Cathodoluminescence Control (CLC-Method): Application to Polymetamorphic Orthogneisses," Chem. Geol. **139**, 287–297 (1997).
48. L. A. Priyatkina and N. N. Lavrovich, "The Geology and Age of the Kalar Gabbro–Anorthosite Massif," in *Early Precambrian of Aldan Shield and Its Frame* (Nauka, Leningrad, 1985), pp. 144–162 [in Russian].
49. O. T. Rämö and I. Haapala, "One Hundred Years of Rapakivi Granite," Mineral. Petrol. **52**, 129–185 (1995).
50. E. B. Sal'nikova, A. M. Larin, A. B. Kotov, *et al.*, "The Kalar Anorthosite–Charnockite Complex of the Aldan–Stanovoi Shield: Age and Tectonic Implications," Stratigr. Geol. Korrel. **12** (3), 3–11 (2004a) [Stratigr. Geol. Correl. **12** (3), 221–228 (2004a)].
51. E. B. Sal'nikova, V. A. Glebovitsky, A. B. Kotov, *et al.*, "Metamorphic Evolution of Granulites from the Kurul'ta Block, Aldan Shield: U–Pb Single Zircon Study," Dokl. Akad. Nauk **398** (2), 1–5 (2004b) [Dokl. Earth Sci. **398**, 968–972 (2004b)].
52. E. B. Sal'nikova, V. P. Kovach, A. B. Kotov, and A. A. Nemchin, "Evolution of the Continental Crust in the Western Aldan Shield: Evidence from Sm–Nd Systematics of Granitoids," Petrologiya **4** (2), 78–93 (1996) [Petrology **5** (2), 105–118 (1996)].
53. V. M. Shemyakin and A. B. Kotov, "The Granitoid Magmatism of the Olekma Foldbelt," in *Early Precambrian of Aldan Shield and Its Frame* (Nauka, Leningrad, 1985), pp. 52–68 [in Russian].
54. J. S. Stacey and J. D. Kramers, "Approximation of Terrestrial Lead Isotopic Composition by a Two-Stage Model," Earth Planet. Sci. Lett. **26**, 207–221 (1975).
55. R. H. Steiger and E. Jager, "Subcomission of Geochronology: Convention of the Use of Decay Constants in Geo- and Cosmochronology," Earth Planet. Sci. Lett. **36** (2), 359–362 (1976).
56. H. J. Stein, J. W. Morgan, R. J. Markey, and J. Wisznewska, "A Re–Os Study of the Suwalki Anorthosite Massif, Northeast Poland," Geophys. J. **20** (4), 111–113 (1998).
57. M. K. Sukhanov and D. Z. Zhuravlev, "Sm–Nd Isotope Age of the Kalar Charnockite–Anorthosite Complex, Eastern Transbaikalia," Geokhimiya, No. 8, 1–5 (2002) [Geochem. Int. **40** (8), 813–817 (2002)].
58. M. K. Sukhanov and P. A. Vaganov, "Genetic Relationships between Silicic and Basic Rocks in the Kalar Charnockite–Anorthosite Massif," Izv. Akad. Nauk SSSR, Ser. Geol., No. 6, 17–31 (1991).
59. M. K. Sukhanov, "The Anorthositic Association of the Kalar Massif," in *Terrestrial and Lunar Anorthosites 1984* (Nauka, Moscow, 1984), pp. 86–111 [in Russian].
60. S.-S. Sun and W. F. McDonough, "Chemical and Isotopic Systematics of Oceanic Basalts: Implications for Mantle Composition and Processes," in *Magmatism in the Ocean Basins*, Ed. by A. D. Saunders and M. J. Norry, Geol. Soc. London, Spec. Publ., No. 42, 313–345 (1989).
61. S. R. Taylor and S. M. McLennan, *The Continental Crust: Its Composition and Evolution* (Blackwell, Oxford, 1985; Mir, Moscow, 1988).
62. D. A. Velikoslavinsky, A. P. Birkis, and O. A. Bogatikov, *The Anorthosite–Rapakivi Association of Eastern European Platform* (Nauka, Leningrad, 1978) [in Russian].
63. V. I. Vinogradov, A. M. Leites, M. I. Buyakaite, *et al.*, "The Rb–Sr System of Rocks in the Olekma–Kalar Anorthosite Massif and Its Northern Surroundings," Dokl. Akad. Nauk SSSR **237** (2), 455–459 (1983).
64. J. B. Whalen, K. L. Currie, and B. W. Chappell, "A-Type Granites: Geochemical Characteristics, Discrimination, and Petrogenesis," Contrib. Mineral. Petrol. **95**, 407–419 (1987).
65. R. A. Wiebe, "Proterozoic Anorthosite Complexes," in *Proterozoic Crustal Evolution*, Ed. by K. C. Condie (Elsevier, Amsterdam, 1992), pp. 215–261.
66. R. Zartman and B. R. Doe, "Plume Tectonics: The Model," J. South Am. Earth Sci. **75**, 135–162 (1981).